20 Jun 2014

X-Ray Digital Industrial Radiography (DIR) for Local Liquid Velocity (VLL) Measurement in Trickle Bed Reactors (TBRs): Validation of the Technique

K. A. M. Salleh

M. F. A. Rahman

Hyoung-Koo Lee
Missouri University of Science and Technology, leehk@mst.edu

Muthanna H. Al-Dahhan
Missouri University of Science and Technology, aldahhanm@mst.edu

X-ray digital industrial radiography (DIR) for local liquid velocity (V$_{LL}$) measurement in trickle bed reactors (TBRs): Validation of the technique

Khairul Anuar Mohd Salleh,[1,a)] Mohd Fitri Abdul Rahman,[2] Hyoung Koo Lee,[1] and Muthanna H. Al Dahhan[1,2]

[1]*Department of Mining and Nuclear Engineering, Missouri University of Science and Technology, Fulton Hall, 310 W. 14th St., Rolla, Missouri 65409, USA*
[2]*Department of Chemical and Biochemical Engineering, Missouri University of Science and Technology, 143 Schrenk Hall, 400 W. 11th St., Rolla, Missouri 65409, USA*

Local liquid velocity measurements in Trickle Bed Reactors (TBRs) are one of the essential components in its hydrodynamic studies. These measurements are used to effectively determine a reactor's operating condition. This study was conducted to validate a newly developed technique that combines Digital Industrial Radiography (DIR) with Particle Tracking Velocimetry (PTV) to measure the Local Liquid Velocity (V$_{LL}$) inside TBRs. Three millimeter-sized Expanded Polystyrene (EPS) beads were used as packing material. Three validation procedures were designed to test the newly developed technique. All procedures and statistical approaches provided strong evidence that the technique can be used to measure the V$_{LL}$ within TBRs. © *2014 AIP Publishing LLC.* [http://dx.doi.org/10.1063/1.4881679]

I. INTRODUCTION

Trickle Bed Reactors (TBRs), widely known as gas-liquid-solid-type reactors, are fixed beds of particles in which both liquid and gas flow concurrently downward. As they move, they come into contact with not only fixed but also structurally randomized solid particles that act as a catalyst. TBRs are widely used in production of fuels (e.g., low-sulfur fuel oils and high-quality middle-distillate fuels) and lubrication products (e.g., intended for use in extremely cold conditions).[1] TBRs are often used when the catalyst's activity can be maintained over a long period of time.[2] TBRs have a free-volume fraction among the packing (known as porosity or void), allowing liquids to flow freely between the particles. This packing material exists in spherical, cylindrical lumps of irregularly shaped extrudes and granules between 0.1 cm and 3.2 cm.[3–5] A number of hydrodynamic studies (i.e., flow distribution, liquid and gas holdup, pressure drop, liquid velocities, and gas velocities) have been conducted on TBRs.[6,7,3,8–10] In general, as with any other packed-bed type reactor, such studies require various measurement techniques to both probe and visualize the phenomena occurring inside the reactor. Approaches that have usually been used to study the TBRs hydrodynamic state involved mimicking an actual operating condition and scaling down the bed size. Such studies led to the development of Computed Tomography (CT),[11] Laser Doppler Anemometry (LDA),[12] Wire Mesh Sensors (WMS),[13] Magnetic Resonance Imaging (MRI),[14] and more. Studying TBR's behavior helps researchers better understand the reactor itself. This increased knowledge allows them to produce reliable, predictive models while properly scaling and improving not only efficiency but also effectiveness of the system.

A. Liquid velocity measurement in a trickle bed reactor

Liquid velocity measurements have been used in hydrodynamic studies to characterize the fluid flow field in a TBR design.[15,13] These measurements reveal both the liquid flow pattern and the liquid distribution inside the bed. A higher liquid flow rate will produce a uniform liquid flow. It will also improve liquid distribution where the pressure drop will be higher. Previous studies that include both theoretical and experimental data often treat TBR systems as having a homogenous void size throughout the system.[16,17] This assumption leads to a misinterpretation of the actual reactor's performance, often ignoring void complexity while providing only global hydrodynamic values of the flow field. Because both void structure and size are totally random, flow fields become completely different throughout the reactor bed, which necessitate measurement of localized parameters of the reactor. One of those parameters is the liquid velocity in between the porosity (void). The measurement and understanding of between-porosity velocity or local liquid velocity (V$_{LL}$) will not only help increasing the knowledge of catalytic conversion of the reactor but it will also assist researchers to validate models used for hydrodynamic studies, particularly computational fluid dynamic (CFD).[14] Schubert *et al.*[13] suggested that such a measurement technique in a packed bed is still rare, typically existing in one of two ways: either intrusive or non-intrusive. Intrusive methods are obviously not the technique of choice to perform localized measurement because of limited yielding result and obstruction to the natural flow.

Several velocity measurement techniques have been explored in the open literature to identify the best possible technique which can be divided into two components: radiation and non-radiation based techniques. The radiation technique (e.g., magnetic resonance imaging (MRI)) is typically applied based on the limitation posed by non-radiation

a)Electronic mail: kmfgf@mst.edu

techniques;[18,14,15] that is, the reactors used are nearly opaque (not optically transparent). Non-radiation methods, such as wire mesh sensors (WMSs) and thermal anemometry, are usually intrusive to the tested system's nature.[19,20,7]

In measuring the local liquid velocity (V_{LL}) in TBRs with an MRI, Sederman and Gladden[9] performed a three-dimensional (3D) flow study in both liquid-solid and gas-liquid-solid systems. Their measurements indicate the V_{LL} could reach approximately five times that of the inlet velocity or superficial liquid velocity (V_{SL}) for a single-phase type TBR (liquid-solid). The V_{SL} is determined by dividing the water volumetric flow rate (Q) with the empty cross sectional area (A) of the reactor. For a multiphase type TBR (gas-liquid-solid) inside 27 mm diameter bed, the V_{LL} can reach up to 50 times that of V_{SL}.[14] The characteristic of the interstitial flow can be represented by Reynold number (Re). Both liquid and gas Re (L or G) are calculated based on the diameter of the packing and V_{SL}. However, MRI seems to be limited to reactor diameter less than 5 cm (maximum diameter reported was 4.6 cm) for gas-liquid-solid-type V_{LL} measurement,[21,9,22,23] is expensive, and is limited to slightly high pressure and non-metallic designs.[13]

Schubert *et al.*[13] both developed and implemented wire mesh sensors based on the electrical permittivity measurement of trickling liquid or flow rate. The packing consists of 2.5 mm diameter spherical γ-alumina that acts as catalysts inside 10 cm bed diameter. The mode of the interstitial velocities changed as the liquid mass flow rate increased. The illustration on Figure 1 shows the multi-phase type TBR with V_{SL} and V_{LL}.

This work highlights the development of a new method that can be used to measure V_{LL}. It also discusses the validation approaches and results used to prove that such a technique is an applicable and useful measurement tool. The newl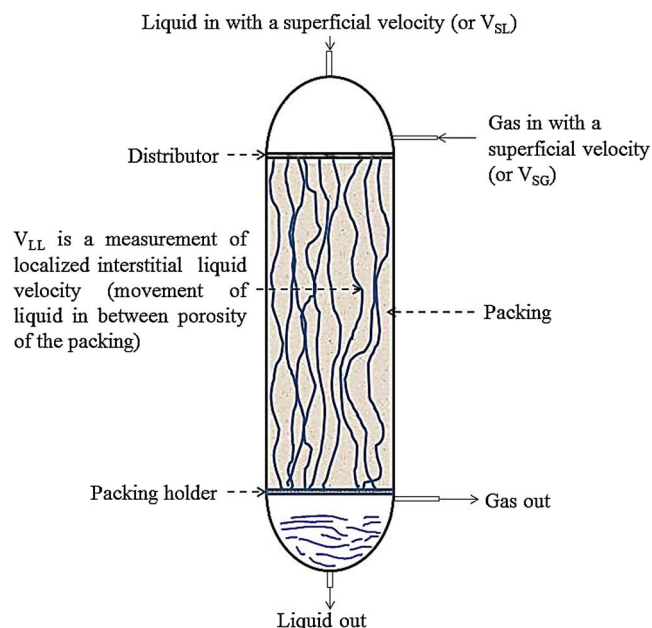y developed technique is designed based on combination of Digital Industrial Radiography (DIR) and Particle Tracking Velocimetry (PTV) techniques. The results gathered from the two-dimensional (2-D) approach represent the first step toward developing three-dimensional (3-D) Digital Industrial X-ray Radiography (DIR) with particle tracking technique (DRPT).

B. Digital industrial radiography

The DIR setup used in this experiment consisted of a Complementary Metal Oxide Semiconductor (CMOS) flat panel X-ray detector and an industrial grade X-ray source. Both computer controllable X-ray generator and a tube (Gulmay, HPX-225-11, UK) with a penetrating energy range between 20 keV and 225 keV, an interchangeable focal spot between 0.4 mm and 1 mm, and a current range between 0 mA and 3 mA were used as the X-ray source. The flat panel X-ray detector (Rad-icon, Shad-o-Box 1024, USA) incorporated a Gd2O2S scintillator screen (Min-R 2190 std.) with a CMOS-type photo diode array. The detector had an active area of 50 mm × 50 mm with a 48 μm pixel pitch, 2.7 fps (370 ms per consecutive frames), a 4000:1 dynamic output. The readout period is 367 ms, and the maximum allowable penetrating energy of 160 keV. The array was protected from ambient light by a carbon-fiber shield.

Both spatial resolution properties and noise characterizations were evaluated with the Modulation Transfer Function (MTF) method. MTF measurements were taken prior to performing V_{LL} measurements. The radiographic exposure parameters used for MTF measurements were the same as those used to determine the V_{LL}. The radiographic exposure parameters included a 635 mm Source Detector Distance (SDD), a 60 kVp penetrating energy and 3 mA current. The estimated MTF was measured with a standard duplex wire image quality indicator (IQI) method (EN 462-5, IE-NDT, England). The performed measurement was free-beam (only the duplex wire was in front of the detector).

Figure 2(a) is a radiographic image of the duplex wire. The spatial resolution measurement was taken when the separation of the wire, representing two intensities (high and low), were close to 20%. Figure 2(b) is a plotted profile line that reveals 28% difference between the two peaks in Figure 2(c). Here, 20% of the modulation ($MTF_{20\%}$) was 6.25 lp/mm (11D). This finding is in agreement with those published by Yagi *et al.*[25] Sinha *et al.*[24] found the MTF to be between 8 lp/mm and 8.5 lp/mm at $MTF_{10\%}$. The measured $MTF_{20\%}$ values suggest that the setup enabled the smallest discernible object to be between 80 μm and 100 μm. More detailed, quantitative evaluations on the same detector model, such as the Noise Power Spectrum (NPS) and the Detective Quantum Efficiency (DQE), are discussed in several publications.[24,25]

C. Laboratory scale setup for trickle bed reactor

The trickle bed reactor setup consisted of a Polyvinyl Chloride (PVC) tube with a 4.5 cm internal diameter and a 40 cm height; it was randomly packed with 3 mm Expanded Polystyrene (EPS) beads up to 30 cm. The beads were not

FIG. 1. Schematic of Trickle Bed Reactor (TBR) with multiphase (liquid and gas) system and their superficial (V_{SL}) and local velocities (V_{LL}).
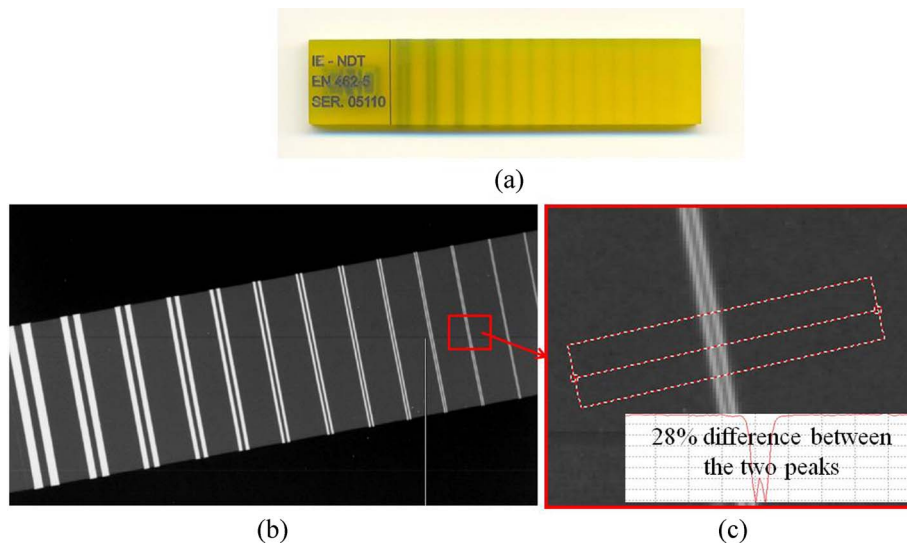
FIG. 2. (a) Double wire IQI, (b) radiographic image of the IQI, and (c) averaged line profile that shows 28% difference between the high and low intensities.

counted during the packing process. These beads were used to mimic catalyst packing as a result of both low atomic number and low density (approximately 25 kg/m^3).[26] The low density EPS beads allowed more penetrating X-rays to reach the CMOS for a better image contrast. This contrast allowed the process of localizing the tracking particles. The bed diameter to particle diameter ratio (15) in this setup is low which promotes wall effects. However, here the focus is to develop the technique and to demonstrate its efficiency in measuring V_{LL} rather than to study the hydrodynamics of a TBR which require minimization on elimination of wall effects by having a ratio of bed diameter to particle diameter larger than 20.[27,28,3]

Deionized water (with a constant temperature 70 ($\pm$2) °F) was used as the liquid phase and was maintained at 20 psi. It was controlled by needle valves and measured by rotameters (Dwyer Instruments, USA, and Range: 50 ml/min–500 ml/min). Each experiment was performed in continuous mode; the water output was channeled to the drain. A syringe injection port was installed between the needle's valve and the tube's liquid inlet (T-Connector). A computer-controlled syringe pump (NE-1000, New Era Pump Systems, USA) was used to continuously pump (set to 10 ml/min) the tracer particle mixture into the liquid while the main liquid moved at trickle flow. The same computer used to control both the X-ray and the syringe pump was used to acquire DIR images (Image Acquisition, [IAQ]). Figure 3 illustrates the experimental setup used in this experiment. Both liquid and gas pressures were maintained at 20 psi. These numbers were based on both the superficial liquid velocity and the EPS beads diameter (used as packing). All experiments were replicated four times; fresh packing was used each time.

D. Particle isolation and tracking

The particle tracking velocimetry (PTV) method is one of the particle image velocimetry (PIV) modes often used to image systems with low density tracking particles.[29,30] PIV is primarily applicable to high density tracing particles. The PTV technique is simple, powerful, and often used in both the quantitative and qualitative study of flow visualization.[31] It allows localized velocity measurements to be performed in either two-dimensional or three-dimensional formats.[32] In general, PTV is applied in two ways: (1) evaluating the same particles on images with different frames (multiple images with both short interval time and short exposure time), (2) manually measuring the length of the same particle trace formed at one frame (single image with long exposure time).[33] The key stages in PTV measurement in any flow studies are highlighted in Figure 4.

Particle detection, isolation, and registration are collectively known as the pre-processing stage. The particles used in this experiment were 1.9 refractive index Barium Titanate glass beads between 106 μm and 125 μm in size (15% relative difference). Results from the spatial resolution test were used to determine the most appropriate sizes for this test. The specific gravity was 3.8 g/cm^3. Particles that moved together with the flowing liquid were isolated by an image processing procedure, as illustrated in Figure 5, according to their intensities, shapes, and sizes. Matlab R2010a ($\times$64) was used for all procedures.

The isolated particles, represented (on average) as a blob with 3 $\times$ 3 pixel size, were tracked by a radial symmetry of the intensity distribution.[34] By doing so, the location of each unique particle could be identified in every image sequence. This tracking procedure was then used to provide a path of the moving particles. Each distance was divided by 370 ms to obtain each particle's velocity.

II. VALIDATION APPROACHES

A. Particle detection test in two consecutive artificial image frames

Two artificial images, assumed to be consecutive, were used to test the tracking algorithm used in this experiment. Each image contained 20 and 2000 artificial particles and
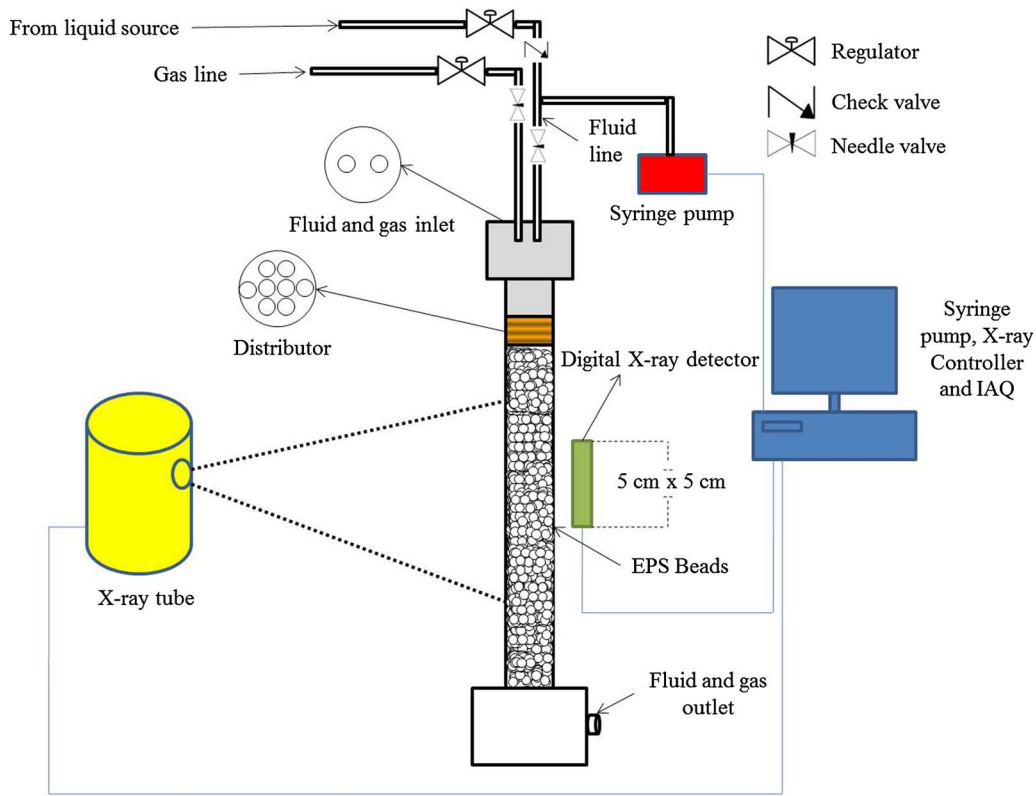
FIG. 3. Experimental trickle bed reactor setup with X-ray tube and detector.
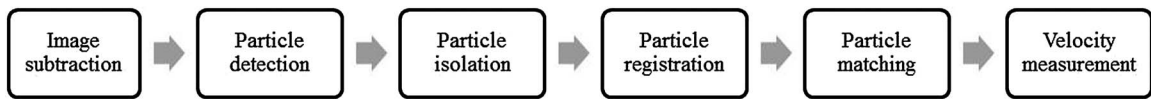

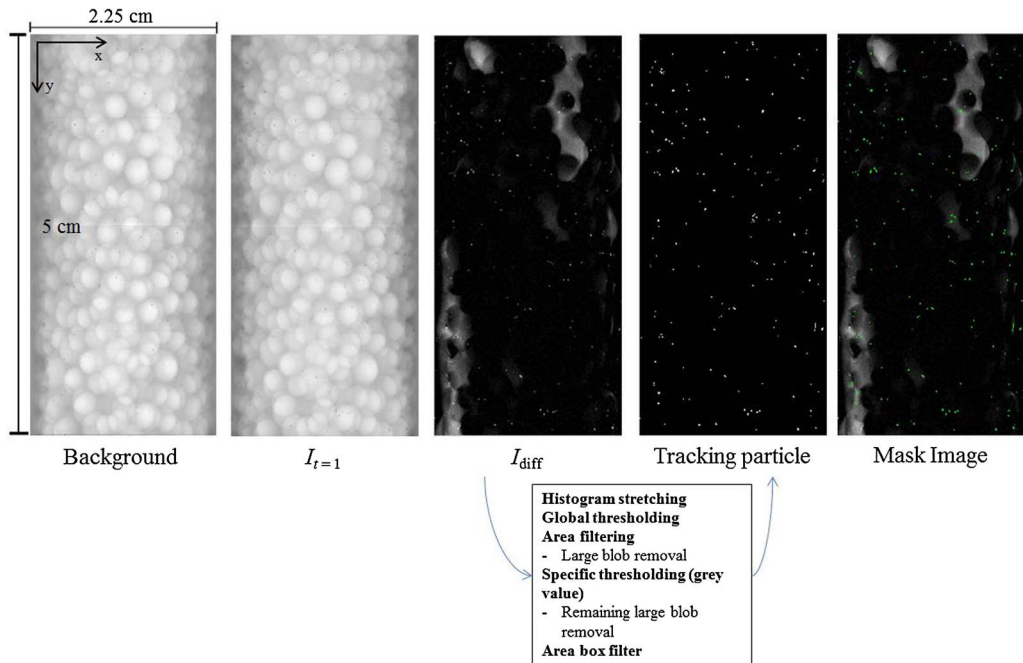FIG. 4. Typical stage in performing PTV measurement.

FIG. 5. Simplified procedure for the particle isolation where $I_{t=1}$ is the first image with tracer particles and I_{diff} is the difference between the image $I_{t=1}$ and the background image.
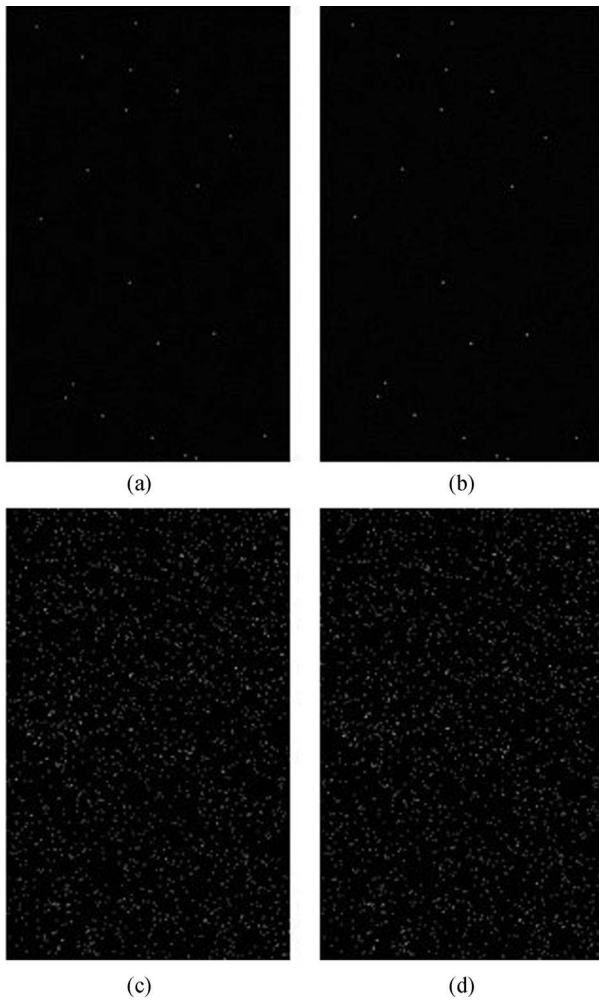
FIG. 6. Images of 586 pixels × 939 pixels. Images (a) and (b) contain 20 artificial particles. Images (c) and (d) contain 2000 particles.

FIG. 7. Plotted vectors for (a) 20 artificial particles with 5 pixel displacement and (b) 2000 particles with 10 pixel displacement.

B. Procedure test on known velocity

The entire procedure, highlighted in Figures 4 and 5, was further tested after the particle detection test was complete by measuring a known velocity. In this test, a syringe, filled with a liquid-tracer particle mixture, was connected to a tube with an internal diameter of 4.25 mm. This tube was placed in front of an X-ray detector so that radiographic images (9.45 mm × 34.3 mm) could be acquired (see Figure 8). The X-ray penetrating energy and current were 40 keV and 2 mA, respectively; the SDD was set to 650 mm. A syringe pump was used to pump the mixture with a constant superficial liquid velocity at 0.0587 cm/s.

This procedure was replicated three times. Figure 9 is an image of the obtained particle path line that traveled with the liquid, inside the empty tube. The color bar indicates the

had a size of 586 pixels × 939 pixels. The artificial tracer particles in both images had a size range of 16.45% difference (106 μm to 125 μm) to mimic the actual tracer particles used in this study. Figure 6 presents the created artificial images that contained the artificial tracer particles moving in a circular direction. The circular motion was obtained by aligning particles with a same size at a specific angle. Images were 8-bit size and the artificial tracer particles were created by adding Gaussian type noise.

Figures 6(a) and 6(b) include images that contain 20 artificial particles (5 max pixel displacements). Figures 6(c) and 6(d) include images with 2000 artificial particles (10 max pixel displacements). All artificial particles were randomly placed. The algorithm highlighted in Sec. I D was successfully applied to show the intended movement of artificial tracer particles. The movement vectors for both artificial tracer particles on each artificial image were plotted in Figure 7. The velocity fields corresponded well to the intended random, circular motion, particularly in Figure 7(b). The vector was clearly defined and plotted on both artificial images. The length of each vector corresponds to the magnitude of pixel displacement.
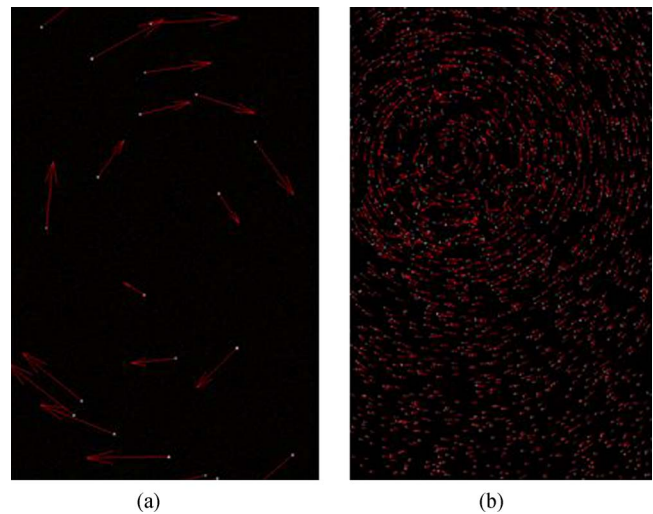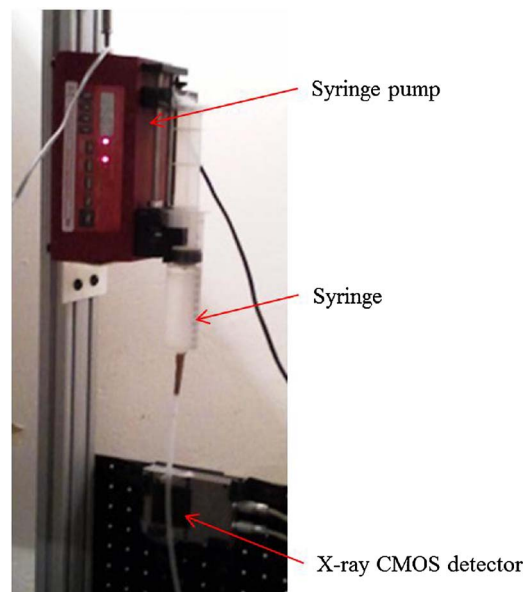

FIG. 8. Syringe containing liquid-tracer particle mixture, syringe pump, and X-ray CMOS detector.
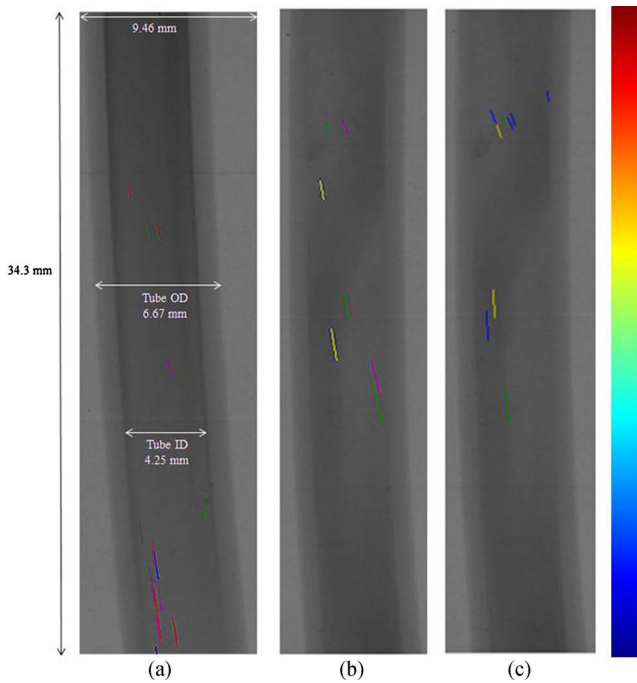
FIG. 9. Three replications of measured velocity [cm/s] inside the tube: (a) 0.049–0.067, (b) 0.052–0.064, and (c) 0.048–0.067.

scale of the particle velocity (which was expected to resemble the travelling liquid velocity). The measured velocity suggests that the proposed procedure produced a difference (either increased or decreased) between the measured velocity and the superficial liquid velocity of at most 16.7% (maximum). Figure 10 illustrates the number of occurrences for the measured particle velocity inside the tube. All radiation exposure works were performed in the Missouri University of Science and Technology Reactor (MSTR). The measured results are presented in Table I.

C. Two-point optical probe for liquid velocity ($V_{LL|OPT}$) measurement

The two point optical probe for liquid velocity measurement technique is developed based on changes in the refractive index of the medium located at the optical probe tip. The
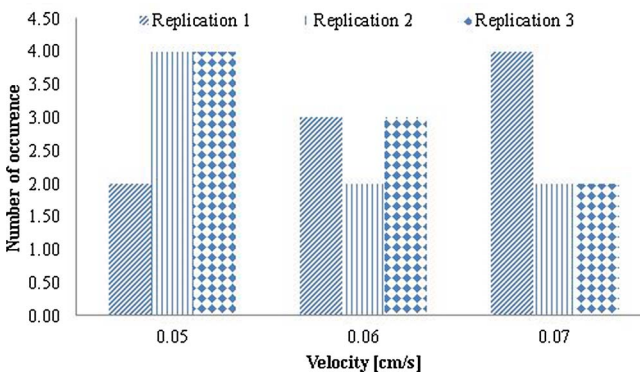

FIG. 10. Number of occurrence of the measured velocity for all replications (T_{test}) with V_{SL} = 0.06 cm/s.

TABLE I. Measured results from three replications.

Superficial liquid velocity (V_{SL}) (cm/s)	Replication	Measured liquid velocity range (cm/s)
0.059	1	0.049–0.067
	2	0.052–0.064
	3	0.48–0.067

two-point optical probe consists of two tips separated by a known distance. The liquid velocity is calculated by dividing the distance between the two tips by the time interval that the liquid takes to pass the two tips. The technique was applied to measure both bubble velocity and bubble behavior in a multiphase system.[35,36] Wu and Ishii[45] sucessfully used this probe to measure the local interfacial area concentration within a bubbly flow. Magaud *et al.*[46] used the dual optical probe technique to detect the local, instantaneous presence of either a liquid or a gas inside a rectangular-type bed.

Conceptually, the measurement technique that uses an optical probe was successfully used to measure the bubble dynamics of a bubble column at Washington University in Saint Louis.[37,38] This probe was manufactured at Missouri University of Science and Technology (Missouri S&T). A 680 nm wave length of light emitted by a Laser Emitting Diode (LED) was transmitted through standard glass fiber connectors and detected by a photodiode.

1. Flow pattern identification

The first steps taken to use two-point optical probe measurement as a validation technique was to identify the flow pattern and measure the V_{LL} of the test bed. In order to that, the new developed combination of particle tracking and DIR technique was applied first. The setup, highlighted in Sec. I C, was used in this experiment. The same tracking material outlined in Sec. I D was used to both visualize and track the flow. The particle identification and algorithm that was successfully used in Secs. II A and II B, respectively, was repeated in this experiment. The superficial liquid and gas velocities (V_{SL} and V_{SG}) used in this experiment were 0.3 cm/s (287 ml/min) and 5.2 cm/s (4963 ml/min), respectively. The location of the optical probe ports used to measure $V_{LL|OPT}$ was divided into three sections. The sections were according to the bed height (Z) and bed diameter (D) ratio (Z/D). These sections (illustrated in Figure 11) were Z/D = 3.3, 3.9, and 4.5.

The DIR used in this study successfully revealed the liquid flow pattern (illustrated in Figure 12). Every velocity of the tracing particles (in the image) is color coded and outliers were removed using one sigma test. These velocities were between 0 cm/s and 16.8 cm/s. The sections from three different Z/D were divided into three smaller sections. These sections were used to position the tip of the optical probe. The center of the smaller sections (indicated by a blue dashed circle), in Figure 13, was marked to indicate the location of the optical probe measurement points. Figure 14 shows histograms
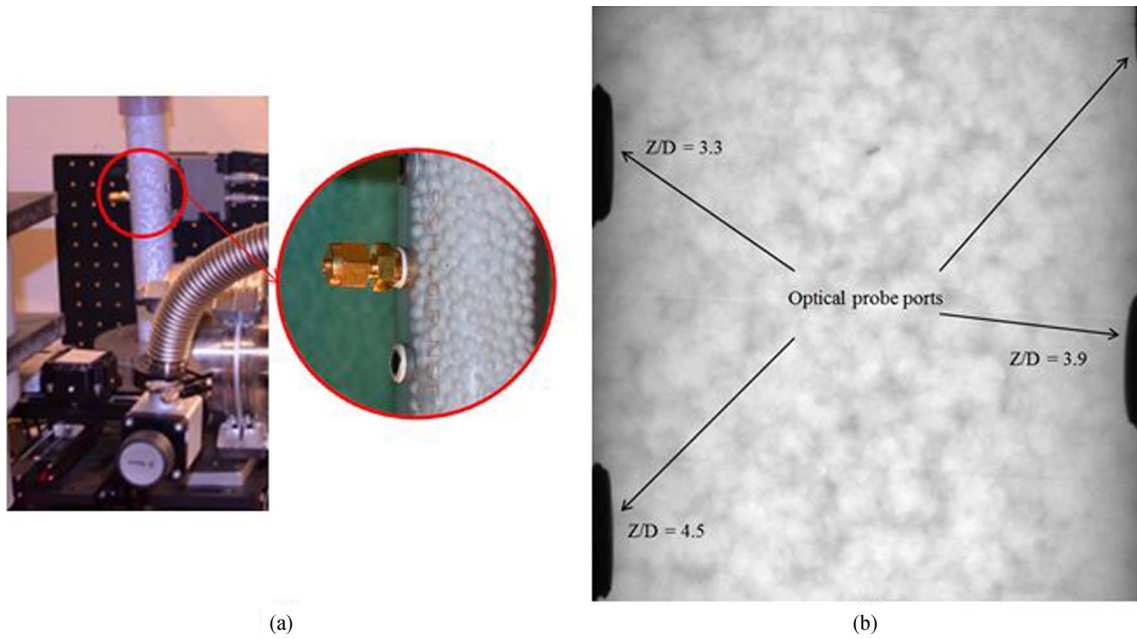
(a)

(b)

FIG. 11. The two-inch TBR setup with (a) fiber optic probe port, and (b) radiographic image with optical probe port located at each Z/D.

of measured V_{LL} with the DIR ($V_{LL|DIR}$). The measurement was replicated three times and Table II lists the V_{LL}'s mean, standard deviation (σ), and variance (σ^2).

2. Two point optical probe measurement ($V_{LL|OPT}$)

The optical probe used in this study (see Figure 15) was an advanced version of the probe originally developed at the Technical University of Delft in the Netherlands.[39] The advanced probe consisted of two tips each with the same length

and diameter. Each fiber consisted of three layers: a quartz glass core having a refraction index of 1.45 and a diameter of 200 μm, a silicon cladding that increased the diameter to 380 μm, and a further protective layer of Teflon, increasing the overall diameter to 600 μm. The entire probe was manufactured in the chemical engineering laboratory at Missouri S&T. Standard glass fiber connectors were used to send a wavelength of 680 nm through a Laser Emitting Diod (LED). This wavelength was then detected by a photodiode. According to Kagumba,[38] due to the difference in refractive index between liquid and the gas phase, when the fiber tip is in a
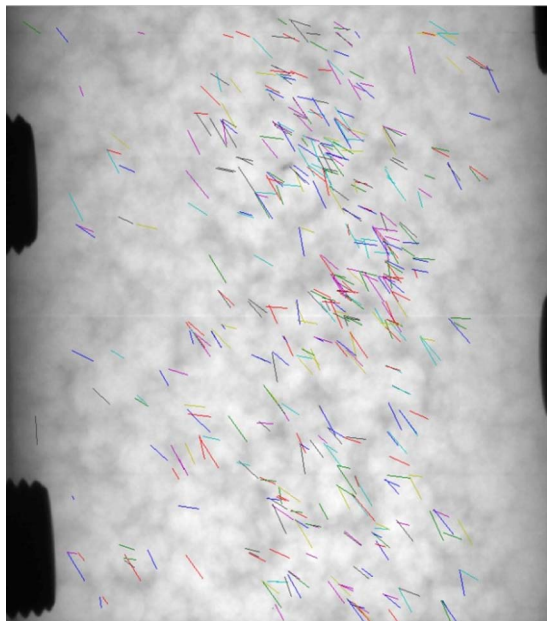

FIG. 12. Flow patterns that were successfully tracked with the combined technique. The color bar indicates the range of obtained V_{LL}.
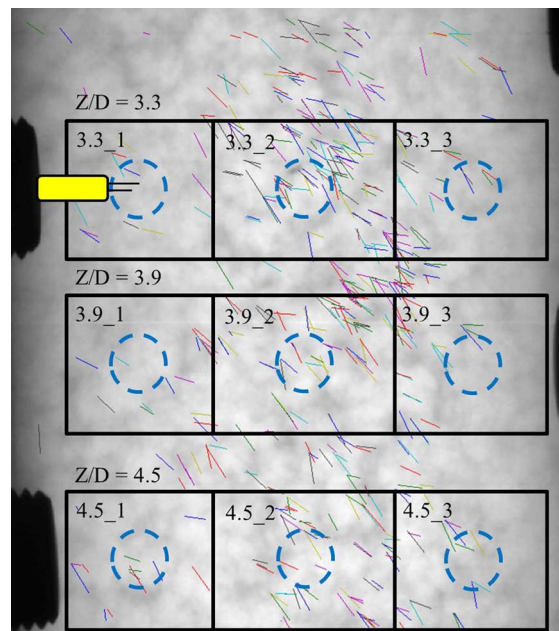

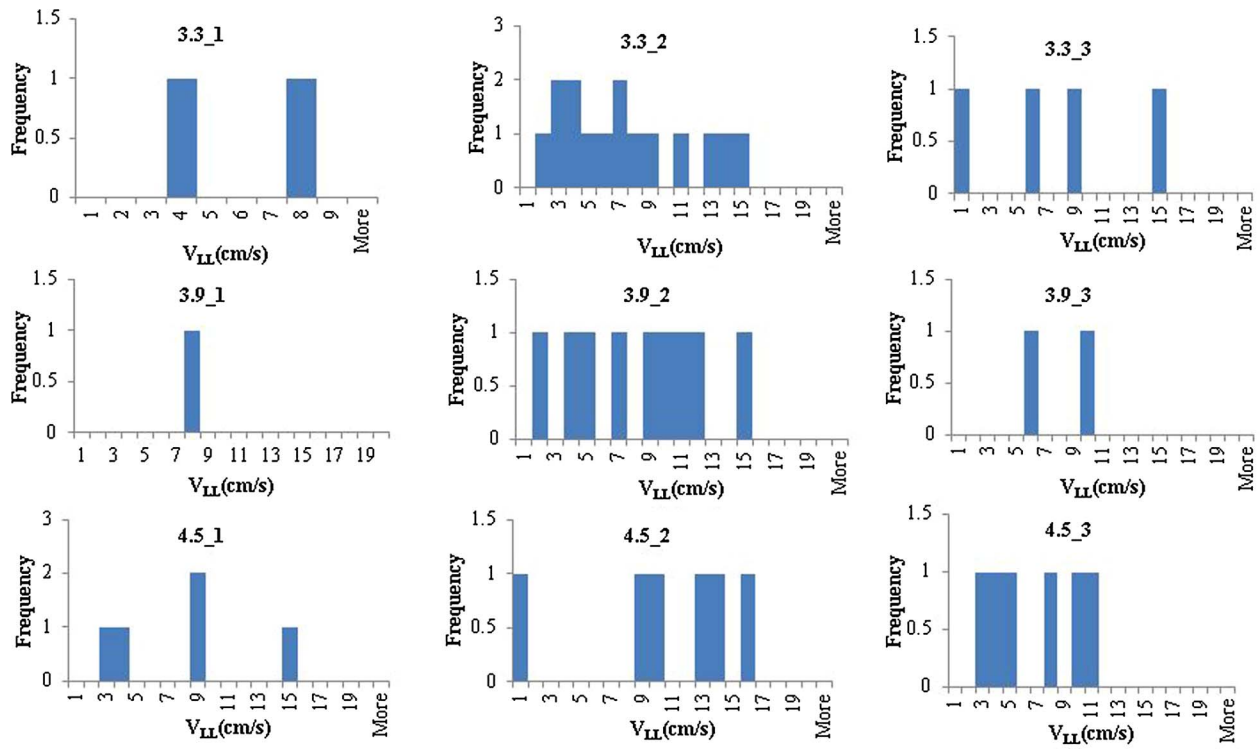FIG. 13. Localized position for the optical probe (blue dashed circle).

FIG. 14. Measured $V_{LL|DIR}$ for each corresponding, localized position (blue dashed circle) listed in Figure 13.

liquid medium, most of the light is refracted into the liquid and very little light is sent back up the fiber. However, when the tip is in the gas bubble, most of the light is reflected, travelling back into the coupler. This coupler then channeled approximately 50% of the reflected light into a photodiode, which finally transformed the light photons into a voltage. The voltage signals (see Figure 16) were collected by a data acquisition board (PowerDAQ PD2- MFS-8-1M/12) at a sampling frequency of 40 kHz. The data acquisition board was purchased from United Electronics Industries. If the liquid is assumed to be constantly flowing in a stable state, the liquid

TABLE II. The mean, standard deviation (σ), and variance of measured $V_{LL|DIR}$ in a two-inch TBR (inside the blue dashed circle).

Location (blue dashed circle)	Mean (cm/s)	σ (cm/s)	Variance
	Z/D = 3.3		
3.3_1	5.49	1.64	2.67
3.3_2	6.97	4.05	16.4
3.3_3	7.46	5.27	27.8
	Z/D = 3.9		
3.9_1	8.12	0	0
3.9_2	8.04	4.08	16.7
3.9_3	7.85	1.97	3.86
	Z/D = 4.5		
4.5_1	7.45	4.6	21.2
4.5_2	9.98	5.06	25.6
4.5_3	6.39	2.97	8.82

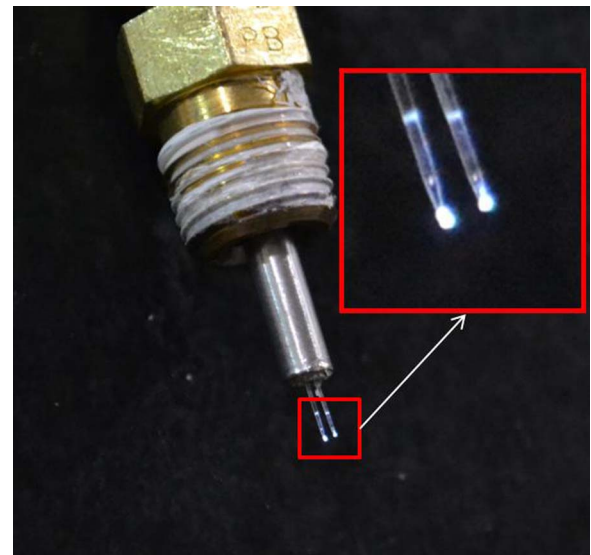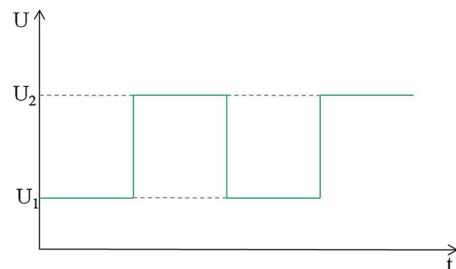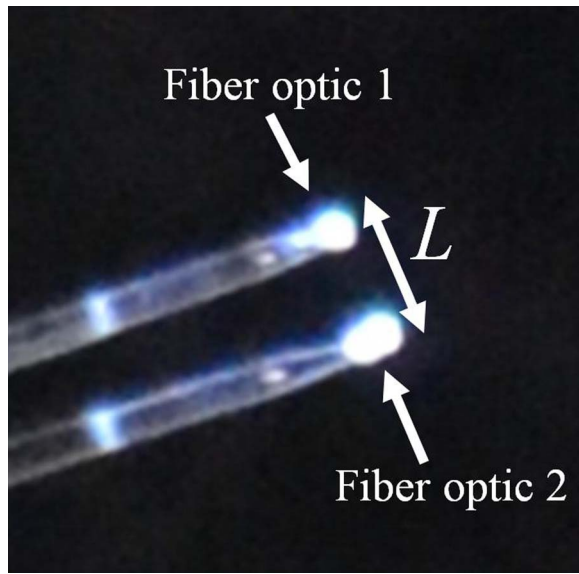FIG. 15. Fiber optic used in this experiment.

FIG. 16. Time series of a single fiber (U1—liquid phase and U2—gas phase).[44]

FIG. 17. The distance, L between fiber optic 1 and fiber optic 2.

velocity ($V_{LL|OPT}$) can be calculated as

$$V_{LL|OPT} = L/\Delta t, \tag{1}$$

where L is the distance between two fiber optics and Δt is the time taken by the liquid to hit fiber optic 1 and fiber optic 2 (see Figure 17).

D. Local liquid velocity results gathered with the optical probe ($V_{LL|OPT}$)

The optical probe was successfully used to measure the local liquid velocity ($V_{LL|OPT}$) inside the two inch TBR. The length of the fiber optic probe was carefully measured before it was placed in approximately, the center of the blue dashed circle. Based on the measured $V_{LL|DIR}$, the tracked liquid is assumed to be the same liquid that hit the fiber optic probe. The superficial liquid and gas velocities used in this experiment were the same as that used in Sec. II D. Table III presents the measured $V_{LL|OPT}$. Three replications were made in every location for proper sampling. Table IV lists the

TABLE III. Average local liquid velocity measured with an optical probe ($V_{LL|OPT}$) at different Z/D levels.

	Position								
	1			2			3		
	$V_{LL\text{-}Avg}$ (cm/s)								
Z/D	Rep 1	Rep 2	Rep 3	Rep 1	Rep 2	Rep 3	Rep 1	Rep 2	Rep 3
3.3	7.55	7.35	7.1	9.3	8.9	8.95	8.7	8.55	8.25
3.9	6.7	6.7	6.45	8.65	8.7	9.35	8.45	8.6	8.25
4.5	8.35	8.1	7.75	6.4	6.9	6.45	8.1	8.05	7.95

TABLE IV. The mean, standard deviation (σ), and variance of measured $V_{LL|OPT}$ in a two-inch TBR (inside the blue dashed circle).

Location	Mean (cm/s)	σ	Variance
	Z/D = 3.3		
3.3_1	7.33	0.18	0.03
3.3_2	9.05	0.18	0.03
3.3_3	8.50	0.19	0.03
	Z/D = 3.9		
3.9_1	6.62	0.12	0.01
3.9_2	8.90	0.32	0.10
3.9_3	8.43	0.14	0.02
	Z/D = 4.5		
4.5_1	8.07	0.25	0.06
4.5_2	6.58	0.22	0.05
4.5_3	8.03	0.06	0.00

basic statistical analysis that was performed on the measured $V_{LL|OPT}$.

E. Hypothesis test (*t*-test with *p*-value < 0.05)

Both measurement results were tested with statistical analysis (*t*-test) to determine their significance levels. *t*-test or Student's *t*-test,[40] equivalent to one-way analysis of variance (ANOVA) with two groups, is a statistical tool to test the difference between means, involving a comparison of a test statistic to the t distribution (*t*-value) to determine the probability of that statistic (*p*-value) if the study's null hypothesis (H_o) is true.[41,42] Conversely, the other hypothesis is known as the alternative hypothesis (H_a). The H_o is either the subject or the technique being referred to or compared to when a new technique is tested. It is a statistical hypothesis that is tested for possible rejection under the assumption that either it is true or it (typically) corresponds to either a general or a default position.[42] The *p*-value is often chosen by its significance level (α). If the *p*-value is smaller than α ($p < \alpha$), the H_o can be rejected at the $\alpha\%$ significance level. A smaller *p*-value provides convincing evidence that H_o is false. A *p*-value a larger α, does not provide enough statistical evidence to reject H_o, it means that there is no enough difference within the samples to conclude a difference (samples are from the same group). Conventionally, the *p*-value is set to be less than 0.05 ($\alpha = 0.05$) driving the H_a to a statistically significant confidence level of 95%.[43] In this validation procedure, the H_o is treated as $V_{LL|OPT}$ while the $V_{LL|DIR}$ as H_a. Statistical analysis software (SAS) was used to perform a *t*-test on both results ($V_{LL|OPT}$ and $V_{LL|DIR}$). The results collected from this *t*-test result are listed in Table V (with $p < 0.05$ to reject H_o). This data suggests that H_o cannot be rejected for most of the measured values when $p < 0.05$. It also reveals an insignificant trend between the measured $V_{LL|OPT}$ and $V_{LL|DIR}$. Of the nine measured locations, only location 3.9_1 was found to have $p < 0.05$. This occurred primarily because only one tracked particle was present in the blue dashed circle. Thus not enough information was gathered to generate more statistical data. Results in Table V suggest that, through hypothesis

TABLE V. Comparison between the mean, standard deviation (σ), variance, degree of freedom (*df*), *t*-value, and *p*-value (α level 0.05) generated by SAS between the measured $V_{LL|OPT}$ and $V_{LL|DIR}$ in a two-inch TBR (blue dashed circle).

Location	$V_{LL|OPT}$			$V_{LL|DIR}$			*t*-test		
	Mean (cm/s)	σ	Variance	Mean (cm/s)	σ	Variance	*df*	*t*	*p*
				Z/D = 3.3					
3.3_1	7.33	0.18	0.03	5.49	1.64	2.67	3	1.5	0.23
3.3_2	9.05	0.18	0.03	6.97	4.05	16.4	16	0.84	0.41
3.3_3	8.50	0.19	0.03	7.46	5.27	27.8	5	0.29	0.78
				Z/D = 3.9					
3.9_1	6.62	0.12	0.01	8.12	0	0	2	9.02	0.01
3.9_2	8.90	0.32	0.10	8.04	4.08	16.7	10	0.33	0.75
3.9_3	8.43	0.14	0.02	7.85	1.97	3.86	6	0.2	0.85
				Z/D = 4.5					
4.5_1	8.07	0.25	0.06	7.45	4.6	21.2	3	0.4	0.72
4.5_2	6.58	0.22	0.05	9.98	5.06	25.6	7	1.02	0.34
4.5_3	8.03	0.06	0.00	6.39	2.97	8.82	7	0.84	0.43

testing, the measured $V_{LL|DIR}$ had more than a 5% chance categorized in the $V_{LL|OPT}$ group.

III. CONCLUSION

Three types of validation approaches were applied to validate newly developed TBR V_{LL} measurement techniques. The first approach used artificial images that contained 20 and 2000 artificial particles of different sizes to test the detection algorithm. Artificial particles' movement was set to be in a circular motion. The newly developed technique successfully identified and tracked each tracer particle's movement. The second approach was performed with a syringe pump set to specific known velocity. A mixture of liquid and tracer particles was injected into a small tube while being irradiate with X-rays. The newly developed particle identification and particle tracing procedures were successfully applied to measure the V_{LL} inside the small tube. The measured velocity and the V_{SL} had a difference of 16.7%. The third approach consisted of using two points fiber optical probe. Both techniques were compared by measuring the V_{LL} inside the same region of interest. Both results were evaluated using Student *t*-test method at $p < 0.05$ and it was found that the measured velocity by using fiber optical probe ($V_{LL|OPT}$) is in the same group as the measured velocity by using combination of DIR and PTV ($V_{LL|DIR}$). Both techniques are found to be complementing each other. Based on these validation procedures and performed statistical analysis, it shows strong evidence that the new developed technique has the accuracy and ability to distinguish, identify, locate, and track the moving seeding particles inside the TBRs. In future investigation, it might be possible to increase the flow rate of the moving liquid. With the increasing V_{SL}, it is expected that less tracer particles can be detected and limitation of such technique can be identified.

[1]M. Dudukovic, F. Larachi, and P. L. Mills, Chem. Eng. Sci. **54**, 1975–1995 (1999).
[2]M. P. Dudukovic, Oil Gas. Sci. Technol. - Rev. IFP **55**, 135–158 (2000).
[3]M. H. Al-Dahhan, F. Larachi, M. P. Dudukovic, and A. Laurent, Ind. Eng. Chem. Res. **36**, 3292–3314 (1997).
[4]A. S. Pushnov, Chem. Pet. Eng. **42**, 14–17 (2006).
[5]G. E. Mueller, Powder Technol. **229**, 90–96 (2012).
[6]W. V. D. Merwe, W. Nicol, and F. D. Beer, Chem. Eng. J. **132**, 47–59 (2007).
[7]C. Boyer and B. Fanget, Chem. Eng. Sci. **57**, 1079–1089 (2002).
[8]M. Schurbet, G. Hessel, C. Zippe, R. Lange, and U. Hampel, Chem. Eng. J. **140**, 332–340 (2008).
[9]A. J. Sederman and L. F. Gladden, Chem. Eng. Sci. **56**, 2615–2628 (2001).
[10]J. Chaouki, F. Larachi, and M. P. Dudukovic, Ind. Eng. Chem. Res. **36**, 4476–4503 (1997).
[11]J. B. Drake and T. J. Heindel, in *Proceedings of the 2009 ASME Fluids Engineering Division Summer Conference*, Vail, CO (ASME, New York, 2009).
[12]P. Therning and A. Rasmuson, Chem. Eng. Sci. **60**, 717–726 (2005).
[13]M. Schubert, A. Khetan, M. J. da Silva, and H. Kryk, Chem. Eng. J. **158**, 623–632 (2010).
[14]M. H. Sankey, D. J. Holland, A. J. Sederman, and L. F. Gladden, J. Magn. Reson. **196**, 142–148 (2009).
[15]C. Boyer, A. M. Duquenne, and G. Wild, Chem. Eng. Sci. **57**, 3185–3215 (2002).
[16]A. J. Sederman, M. L. Johns, A. S. Bramley, P. Alexander, and L. F. Gladden, Chem. Eng. Sci. **52**(14), 2239–2250 (1997).
[17]Q. Chen, W. Kinzelbach, and S. Oswald, J. Environ. Qual. **31**, 477–486 (2002).
[18]U. Kertzscher, A. Seeger, K. Affeld, L. Goubergrits, and E. Wellnhofer, Flow Meas. Instrum. **15**, 199–206 (2004).
[19]W. Wangjiraniran, Y. Motegi, S. Richter, H. Kikura, M. Aritomi, and K. Yamamoto, J. Nucl. Sci. Technol. **40**(11), 932–940 (2003).

[20]C. Marcandelli, G. Wild, A. S. Lamine, and R. Bernard, Chem. Eng. Sci. **54**, 4997–5002 (1999).

[21]L. F. Gladden and A. J. Sederman, J. Magn. Reson. **229**, 2–11 (2013).

[22]M. L. Johns, A. J. Sederman, A. S. Bramley, and L. F. Gladden, AIChE J. **46**(11), 2151–2161 (2000).

[23]A. J. Sederman, M. L. Johns, P. Alexander, and L. F. Gladden, Chem. Eng. Sci. **53**(12), 2117–2128 (1998).

[24]V. Sinha, A. Srivastava, H. K. Lee, and X. Liu, in *Aerospace Engineering, Civil Infrastructure, and Homeland Security 2013*, San Diego (SPIE, 2013).

[25]N. Yagi, M. Yamamoto, K. Uesugi, and K. Inoue, AIP Conf. Proc. **705**, 885–888 (2004).

[26]M. G. Basavaraj, G. S. Gupta, K. Naveen, V. Rudolph, and R. Bali, AIChE J. **51**(8), 2178–2189 (2005).

[27]A. Atta, S. Roy, and K. D. P. Nigam, Chem. Eng. Sci. **62**, 7033–7044 (2007).

[28]A. Attou, C. Boyer, and G. Ferschneider, Chem. Eng. Sci. **54**, 785–802 (1999).

[29]R. J. Adrian, Annu. Rev. Fluid Mech. **23**, 261–304 (1991).

[30]R. Theunissen, MS thesis, University of Technology Delft, Delft, 2003.

[31]Y. A. Hassan, T. K. Blanchet, and C. H. Seeley, Jr., Meas. Sci. Technol. **3**, 633–642 (1992).

[32]K. Ohmi and H. Y. Li, "Particle-tracking velocimetry with new algorithms," Meas. Sci. Technol. **11**, 603–616 (2000).

[33]C. Liu and L. Tao, J. Coastal Res. **50**, 415–419 (2007).

[34]R. Parthasarathy, Nat. Methods **9**(7), 724–726 (2012).

[35]W. H. Park, W. K. Kang, C. E. Capes, and G. L. Osberg, Chem. Eng. Sci. **24**(5), 851–865 (1969).

[36]G. R. Rigby, G. P. van Blockland, W. H. Park, and C. E. Capes, Chem. Eng. Sci. **25**(11), 1729–1741 (1970).

[37]J. Xue, Ph.D. thesis, Washington University, Saint Louis, 2004.

[38]J. Xue, M. Al-Dahhan, M. P. Dudukovic, and R. F. Mudde, Flow Meas. Instrum. **19**, 293–300 (2008).

[39]M. O. O. Kagumba, Ph.D. thesis, Missouri University of Science and Technology, Rolla, 2013.

[40]R. R. Wilcox, *Introduction to Robust Estimation and Hypothesis Testing*, 3rd ed. (Academic Press, Massachusetts, 2012).

[41]S. Boslaugh, *Statistics in a Nutshell*, 2nd ed. (O'Reilly Media, California, 2012).

[42]T. M. Cabral and R. M. Rangayyan, *Fractal Analysis of Breast Masses in Mammograms* (Morgan and Claypool Publishers, California, 2012).

[43]S. C. Albright, W. L. Winston, and C. Zappe, *Data Analysis and Decision Making*, 3rd ed. (Thomson Higher Education, Ohio, 2006).

[44]C. Meitzner, Diploma thesis, TU Dresden, Dresden, 2011.

[45]Q. Wu and M. Ishii, Int. J. Multiphase Flow **25**, 155–173 (1999).

[46]F. Magaud, M. Souhar, G. Wild, and N. Boisson, Chem. Eng. Sci. **56**, 4597–4607 (2001).